An Improved CenterNet Method for Wing Icing Detection

WANG Yifan[1], *WEI Jiatian*[1], *ZUO Chenglin*[2*], *ZHOU Wenjun*[1], *XIONG Hao*[2], *ZHAO Rong*[2], *PENG Bo*[1], *WANG Yang*[1]

1. School of Computer Science, Southwest Petroleum University, Chengdu 610500, P.R. China;
2. Key Laboratory of Icing and Anti/De-icing of China Aerodynamics Research and Development Center, Mianyang 621000, P.R. China

(Received 27 March 2023; revised 30 October 2023; accepted 28 November 2023)

Abstract: Aircraft wing icing detection is a crucial task during high-altitude flights because ice accumulation on the leading edge of wings can change their aerodynamic shape and reduce lift capacity. This paper proposes a rotated object detection method called RA-CenterNet, based on the CenterNet model, to overcome the limitations of existing icing detection approaches that either rely on operator experience or require high engineering implementation and hardware development costs. To address the specific icing area directions presented in wind tunnel experimental datasets, a novel angle prediction branch network that enables precise calibration of rotated targets is designed. Additionally, the convolutional block attention module (CBAM) is incorporated to enhance the feature extraction ability of the neural network for ice-shaped boundaries. Comparative experiments are conducted to validate the performance of the proposed method against other rotated object detection approaches and the baseline network. The results demonstrate that our RA-CenterNet method has a significant competitive advantage over the mainstream rotation-based object detection algorithms.

Key words: wing icing; deep learning; rotated target detection; anchor-free; attention mechanism

CLC number: TP391 **Document code:** A **Article ID:** 1005-1120(2023)06-0703-11

0 Introduction

Ice formation is common when an aircraft is flying at high altitudes and comes into contact with water vapor or condensation in the air. The ice primarily accumulates on the windward surface of the aircraft, including wings, front windshield, engine air inlet, and tail. However, the wings, responsible for providing 60% to 80% lift to the aircraft, are particularly susceptible to ice accumulation. Ice accumulation on the wings changes their aerodynamic shape, leading to a decrease in lift and an increase in drag. Uneven ice accumulation on the wings or ice accumulation at different locations can also change the aircraft's center of gravity, thereby affecting its control stability and even causing structural freezing and loss of control. As such, detecting ice on aircraft wings is crucial for ensuring safe flight.

Currently, two commonly used methods for detecting icing on aircraft wings are visual and electronic detection[1]. Wing visual detection relies on the observation of the crew under spotlights illumination, which lacks sufficient accuracy and depends on observer experience. Electronic detectors are typically single-point detection structures and are not suitable for detecting regional icing, which requires multiple icing sensors to be installed. Although array sensors can detect regional icing, they entail high engineering implementation and hardware development costs[2]. Furthermore, from the perspective of wing structural and system design, the position of the wing fuel tank limits the coverage of all important components positions by the icing detection device[3]. In addition, the installation of most icing detection equipment requires changes to the air-

*Corresponding author, E-mail address: zuochenglin@cardc.cn.

How to cite this article: WANG Yifan, WEI Jiatian, ZUO Chenglin, et al. An improved CenterNet method for wing icing detection[J]. Transactions of Nanjing University of Aeronautics and Astronautics, 2023, 40(6): 703-713.

http://dx.doi.org/10.16356/j.1005-1120.2023.06.007

craft's structural shape, which further complicates equipment installation[4]. These limitations highlight the need for a new and effective wing icing detection system capable of automatically locating icing regions. Such a system would essentially involve object detection, and computer vision is perfectly suitable to this task.

The development of an icing detection system involves the design and experimentation of the system in a wind tunnel, where the experimental wings are subjected to the same environmental conditions as real flights. Unlike typical horizontal object detection tasks, the analysis of the concentrated icing region's target shape in wing icing experiments exhibits distinctive characteristics. Firstly, the region displays a high length-to-width ratio, with experimental data indicating that icing regions primarily form at the wing's leading edge and shaped as vertically or diagonally elongated rectangles. Secondly, due to the wing's inclination angle, icing regions attached to its surface display a certain inclination angle.

Based on the aforementioned characteristics, conventional methods for detecting horizontal frames tend to capture more redundant background information, which is suboptimal for precise target calibration. To address this issue, this paper proposes a new approach called RA-CenterNet, which is a rotated target detection method based on CenterNet[5]. RA-CenterNet predicts the position of the target's center point, as well as its width, height, offset, and the rotation angle of the detection box. By utilizing this approach, our detection achieves more accurate identification and calibration of wing icing targets.

This paper presents two significant contributions. Firstly, to overcome the issue of specific icing area directions presented in wind tunnel experimental datasets, we propose a novel angle prediction branch network. This network allows for precise calibration of rotated targets, thus addressing the aforementioned challenge. Secondly, to overcome the challenge of background noise affecting target feature information during the convolution process, and the difficulty in identifying the blurred icing boundary of the wing, we introduce the convolutional block attention module (CBAM)[6] into the backbone network. This significantly enhance the feature extraction ability of the network's output feature map. Finally, we apply skip connections to the feature maps with the same resolution, which provides more detailed and effective feature information for the icing target detection task without compromising the network's prediction performance.

1 Related Work

1.1 Aircraft icing detection technology

Currently, there are several methods commonly used for detecting aircraft icing, including mechanical, optical, and neural network approaches[7]. A notable example of a mechanical icing detector is the flat film resonant sensor developed by the Vibro-Meter Company in Sweden[8]. Meanwhile, the optical method has been extensively researched, with the fiber optic icing sensor operating by detecting the energy loss resulting from the reflection and scattering of infrared energy by ice. This allows the system to determine the extent of icing based on changes in signal amplitude. With its small size, high sensitivity, and wide measurement range, the fiber optic icing detection system can be conveniently installed in various parts of an aircraft, making it a competitive new generation of icing sensors[9].

Improving the detection performance of single-point sensors is undoubtedly important, but the detection of icing surfaces over a large area and region is also a critical area of research in aircraft icing detection[10]. At present, the visual method[11] is commonly used because of its low cost and convenience for the crew to check the windshield and wing icing conditions using wing searchlights and icing probes. However, this method relies on empirical judgment and lacks a scientific basis. To address this issue, Ref.[12] proposed a machine learning method based on hyperspectral and multispectral images for detecting ice shapes on the aircraft surface. Their research demonstrated the effectiveness of machine learning in recognizing wing icing, which represents an exciting development in this field.

1.2 Object detection technology

Prior to the emergence of deep learning, traditional algorithms played a significant role in the field of object detection, and many outstanding algorithms were proposed. Viola and Jones[13] were the first to combine Haar features and cascade structure for extracting features and detecting faces in real-time, which solved the inefficiency problem caused by sliding window. Dalal and Triggs[14] proposed gradient histogram features and combined them with linear SVM classifiers for pedestrian detection, achieving high detection accuracy. Lowe[15] used the SIFT algorithm to find feature points and match targets, thereby improving the recognition rate of occluded targets. Bay et al.[16] proposed the SURF algorithm, which was based on the SIFT algorithm and used an approximate Hessian matrix to reduce the downsampling process and improve detection speed.

Deep learning methods for object detection are generally classified into two categories: Anchor-based methods and anchor-free methods. Anchor-based methods, such as the R-CNN series[17-19], have achieved remarkable success in detecting objects in natural scene. These methods initially extract candidate regions in the input image where the object may exist and subsequently perform classification and regression operations on these regions to obtain the object's detection box. Although these methods offer high detection accuracy, the generation of anchors necessitates the manual tuning of numerous parameters and additional post-processing operations, resulting in a high model complexity and computational demands. Moreover, a significant proportion of anchor regions serve as negative samples, which can lead to an imbalanced distribution of positive and negative samples, making it challenging to train the model.

Law et al.[20] proposed CornerNet, an anchor-free target detection method that achieved an average accuracy of 42.1% on the COCO dataset[21], surpassing all previous one-stage detectors. However, its detection speed was significantly slower than YOLO[22]. To improve the CornerNet method, Zhou et al.[5] introduced an additional key point at the center of the target, enabling more precise corner point matching. The anchor-free series of algorithms have a smaller network complexity and calculation load, enabling CenterNet to strike a balance between detection accuracy and speed.

2 RA-CenterNet Algorithm

While the CenterNet algorithm has shown promising results on the MSCOCO dataset, detecting targets in the wind tunnel experimental dataset through this approach presents significant challenges due to the high aspect ratios, tilted angles, and limited differences in edge information. As a result, in order to improve the network's adaptability to wing icing images and enhance detection accuracy, modifications must be made to the CenterNet network using a more appropriate approach.

2.1 Principle of CenterNet algorithm

CenterNet is an anchor-free object detection algorithm that is based on the CornerNet approach[20], and its network architecture is shown in Fig.1, where w and h denote the width and the height. The core idea of this algorithm is to treat an object as a keypoint, which represents the center of the objects' bounding box. By estimating the keypoint, the algorithm can localize the object's center and predict other attributes, such as size, 3-D position, and human pose information. Compared to other two-stage object detection algorithms, CenterNet eliminates the need for time-consuming and computationally expensive anchor operation, resulting in improved detection performance. Additionally, the algorithm performs filtering directly on the heatmap, eliminating the need for non-maximum suppression (NMS) and further enhancing its speed. CenterNet employs ResNet[23], Hourglass[24], and DLA[25] as backbone networks for feature extraction, which includes deconvolutional layers for information extraction and improved spatial resolution. The output layer consists of three prediction branches: Keypoint heatmap prediction, keypoint offset prediction, and object size prediction. Consequently, the loss function comprises three components,

shown as

$$L_{\text{det}} = L_{\text{k}} + \lambda_{\text{size}} L_{\text{size}} + \lambda_{\text{off}} L_{\text{off}} \tag{1}$$

where L_{det} is the overall loss value, comprising three components: L_{k} for the keypoint heatmap prediction loss, L_{off} for the keypoint offset loss, and L_{size} for the target width and height loss. Specifically, the weighting factors for L_{size} and L_{off} are $\lambda_{\text{size}}=0.1$, $\lambda_{\text{off}}=1$, respectively.

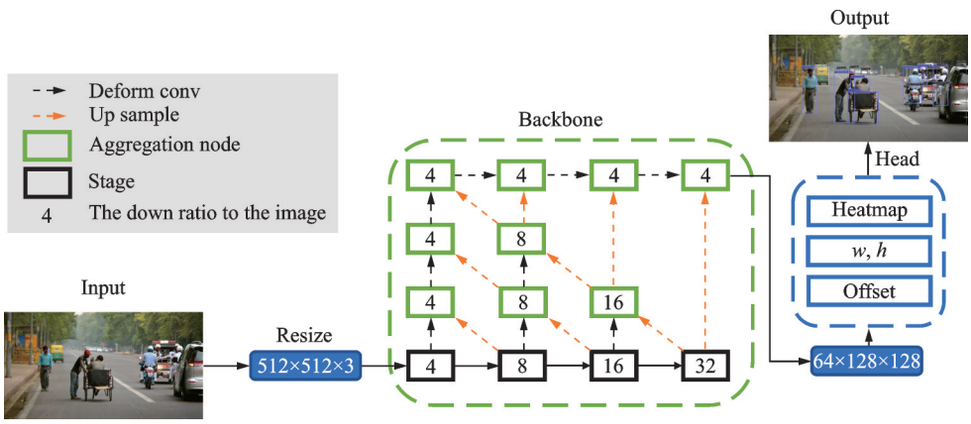

Fig.1 CenterNet network architecture

2.2 RA-CenterNet network design

The regression box predicted by the CenterNet algorithm comprises four parameters, namely x, y, w, and h. Here, x and y represent the coordinates of the regression frame's center point.

This paper proposes an additional parameter, θ, for angle regression to represent the rotated box. The bounding box is expressed as (x, y, w, h, θ). However, the periodicity of the angle can cause different numerical values representing the same angle, which can cause ambiguity. To address this issue, we adopt a method similar to the OpenCV representation. Specifically, we restrict the angle range of the rotation frame to a specific range to eliminate ambiguity, as shown in Fig.2.

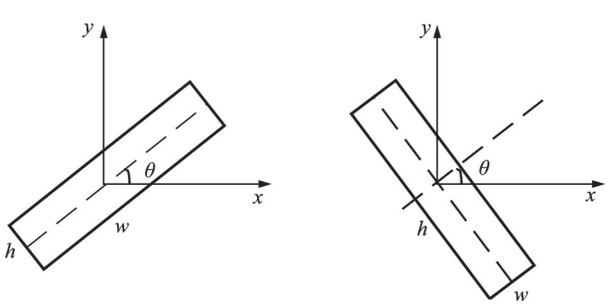

Fig.2 Spin box representation method($\theta\in(-\pi/4, \pi/4]$)

In order to restrict the range of angle output in the angle prediction branch network, the hyperbolic tangent function is employed as the activation function in this study. With a range bounded between $+1$ and -1 and an origin value of 0, this function is highly suitable for the angle range of the rotating box utilized in this research. Eq.(2) defines the activation function, with a multiplication of $\pi/4$ before the hyperbolic tangent function to constrain the angle.

$$f(x) = \frac{\pi}{4} \times \frac{e^{x} - e^{-x}}{e^{x} + e^{-x}} \tag{2}$$

This study addresses the limitations of the original CenterNet[5] algorithm in detecting rotated targets by integrating the angle branch prediction network. Additionally, the CBAM module[6] is introduced to enhance the correlation of target features in the icing area, with regard to both dimensions and spatial positions. This significantly improves the neural network's capacity to extract features along the ice-shaped boundaries. The enhanced CenterNet algorithm comprises two parts, and its network structure is depicted in Fig.3.

(1) Feature extraction part. The feature extraction process employed in this study utilizes the DLA-34 backbone network, which has been enhanced through the integration of skip connections. These connections facilitate the merging of deep high-level semantics with shallow fine information in the channel dimension. Furthermore, to generate a feature map containing the deepest information

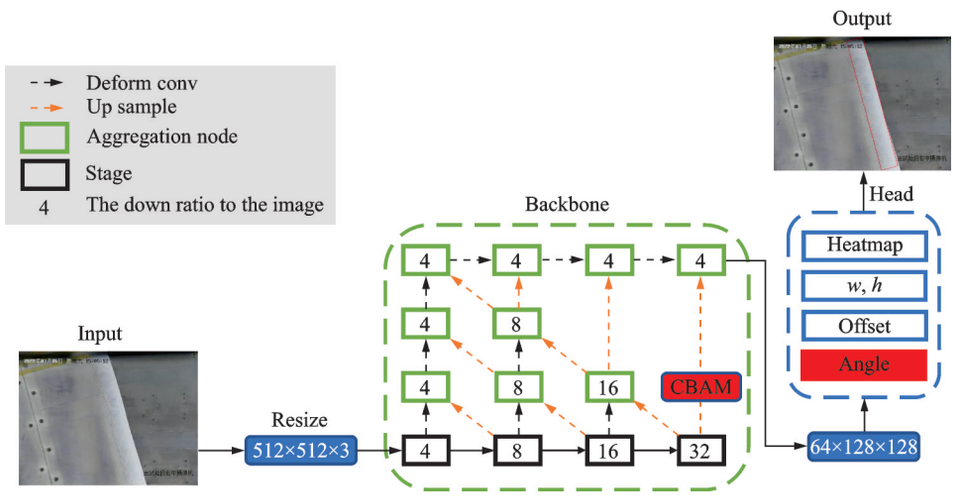

Fig.3 RA-CenterNet network architecture

and exhibiting strong abilities to generalize and abstract features, the CBAM module is applied to the DLA network[25]. As a result, this feature map has the largest number of fusion channels.

(2) Prediction of branch network part. The upsampled and fused feature maps undergo processing through four branch networks, consisting of 3×3 and 1×1 convolutions. These networks generate a keypoint heat map measuring 128×128×C, where C represents the number of target categories (in this study, C=1). Alongside the heat map, the networks produce center point offset information of size 128×128×2 and angle information of size 128×128×1.

2.3 CBAM attention module

The attention mechanism has become a pivotal tool in various data processing tasks, such as natural language processing and image recognition. By utilizing a distinct data processing technique, it enables networks to identify the most salient features within images or text, thereby emphasizing relevant information. Currently, there are three primary types of attention mechanisms: Channel attention, spatial attention, and spatial and channel mixed attention. Regarding the icing data set, which exhibits a high aspect ratio and small edge information difference, the attention mechanism proves to be highly effective in detecting target features within the icing area of an image while suppressing non-target features, such as non-icing areas on the wing. Consequently, the accuracy of detection is significantly improved.

This article selects the CBAM approach[6], which utilizes a mixed attention mechanism that combines both spatial and channel attention. The CBAM module comprises two sub-modules, the channel attention module (CAM) and the spatial attention module (SAM), which are responsible for enhancing important image features in the channel and spatial dimensions, respectively. A visual representation of the CBAM module architecture is depicted in Fig.4.

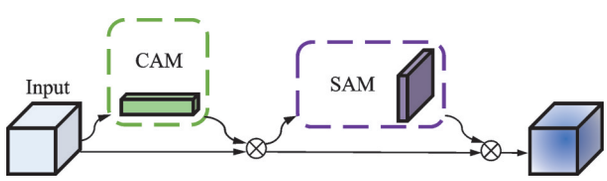

Fig.4 CBAM module architecture

The overall architecture of the RA-CenterNet network utilizes DLA-34 as the backbone network and employs four down-sampling stages to extract deep features. To mitigate the negative impact of background noise on target feature information during the convolution process, CBAM is incorporated after down-sampling to enhance the network's attention on potential target regions. However, the 512 channels in the backbone network of RA-CenterNet do not all contain meaningful information. To address this issue, the CAM channel attention module is introduced to reduce the correlation of less useful and less meaningful channels and select

more practical and meaningful channels. To generate channel attention maps A_c, the feature map $\boldsymbol{M} \in \mathbf{R}^{C \times H \times W}$ is processed through two pooling branches and then fed into a three-layer neural network to obtain two $C \times 1 \times 1$ vectors that are subsequently added together. Finally, the sigmoid function is used to restrict the values of A_c within the range (0, 1), shown as

$$A_c = \Delta\big(\mathrm{MLP}\big(\mathrm{MaxPool}(\boldsymbol{M})\big) + \mathrm{MLP}(\mathrm{AvgPool}(\boldsymbol{M}))\big) \tag{3}$$

where MLP processes pooled features to learn channel relationships and generates weights for recalibrating the input feature map.

In our method, a SAM spatial attention module is employed to reduce the correlation of irrelevant background and coordinates with low semantic meaning, and to select more practical coordinate ranges that cover objects. This is accomplished by obtaining a feature map $\boldsymbol{M}'$ with focused channels via element-wise multiplication between A_c and $\boldsymbol{M}$, shown as

$$\boldsymbol{M}' = \boldsymbol{M} \otimes A_c(\boldsymbol{M}) \tag{4}$$

The feature map $\boldsymbol{M}'$ is then globally pooled along the channel axis twice, followed by a 7×7 convolution and sigmoid activation to ensure that the values of the output spatial attention map A_s are confined to the interval (0, 1), shown as

$$A_s = \Delta\big(f^{7\times 7}(\mathrm{MaxPool}(\boldsymbol{M}'); \mathrm{AvgPool}(\boldsymbol{M}'))\big) \tag{5}$$

The final output $\boldsymbol{M}''$ with focused positions is obtained by element-wise multiplication between A_s and $\boldsymbol{M}'$, shown as

$$\boldsymbol{M}'' = \boldsymbol{M}' \otimes A_s(\boldsymbol{M}') \tag{6}$$

By means of this approach, more refined and effective feature information, such as gradients, is provided for ice target detection tasks, without compromising the network's predictive performance. The skip connections are used to connect the obtained feature maps with the same resolution, thereby refining the center and edge positions of the detection results. Overall, the attention mechanism proposed in this study contributes to improving the accuracy of object detection and enhancing the quality of the feature maps generated by the network.

2.4 Angular prediction loss

The RA-CenterNet algorithm leverages the loss function of CenterNet. Specifically, the rotation angle loss function, denoted by $\hat{A}_{p_k}$ for the predicted deviation angle of the detection box output by the model and a_k for the true rotation angle of the target, the loss is shown as

$$L_{\mathrm{angle}} = \frac{1}{N}\sum_{k=1}^{N}\left|\hat{A}_{p_k} - a_k\right| \tag{7}$$

The overall loss is defined as

$$L = L_{\mathrm{k}} + \lambda_{\mathrm{size}}L_{\mathrm{size}} + \lambda_{\mathrm{off}}L_{\mathrm{off}} + \lambda_{\mathrm{angle}}L_{\mathrm{angle}} \tag{8}$$

Following experimentation, the optimal parameter values are determined to be $\lambda_{\mathrm{size}}=0.1$, $\lambda_{\mathrm{off}}=1$, $\lambda_{\mathrm{angle}}=0.1$.

3 Experiment and Result Analysis

In order to validate the effectiveness of the RA-CenterNet algorithm, we conducted comparative experiments with other rotated object detection methods, namely Rotated Faster R-CNN[26], Beyond Bounding-Box[27], SASM[28], Oriented RepPoints[29], as well as the original CenterNet algorithm[5]. Moreover, we performed ablation experiments on the RA-CenterNet algorithm to assess the impact of different structural modifications on detection performance improvement.

3.1 Experiment settings

The experiments are conducted on Ubuntu 20.04 operating system using PyTorch 1.7.0 and CUDA version 11.0, with an NVIDIA RTX 3080 GPU and an AMD 5800X CPU.

The data used in this study consists of images captured from various angles during an icing wind tunnel experiment, which replicates the conditions of an aircraft passing through a cloud of supercooled water droplets by adjusting the water and air pressure of the nozzle. The dataset comprises 241 images in the training set and 239 images in the validation set.

This paper employs random flipping, scaling, and cropping as data augmentation techniques and adopts Adam as the optimizer to optimize the overall objective. During training, the batch size is set to 8, epoch is set to 200, and the initial learning rate is

set to 0.000 125. The learning rate schedule decreases by a factor of 10 at epochs 90 and 150 to stabilize the training process.

3.2 Analysis of results

3.2.1 Comparison of experimental results and analysis

The algorithm proposed in this study is trained and tested on the same dataset as the CenterNet algorithm and several mainstream rotation-based object detection networks. The results are presented in Table 1.

Table 1 Comparison of experimental results of different algorithms

Algorithm	Average precision/%	Frame rate/(frame•s^{-1})
Beyond Bounding-Box	69.6	5.5
Rotated Faster R-CNN	76.1	3.8
Oriented RepPoints	79.0	4.3
SASM	85.8	4.8
CenterNet	70.2	**11.38**
Ours	**92.7**	9.47

Table 1 shows that the proposed RA-CenterNet algorithm achieves detection accuracy improvements of 16.6%, 23.1%, and 13.1%, respectively, compared with the two-stage Rotated Faster R-CNN, the two-stage-like Beyond Bounding-Box, and Oriented RepPoints algorithms. Moreover, compared with the SASM algorithm, the proposed algorithm achieves a detection accuracy improvement of 6.9%. In comparison with the original CenterNet algorithm, RA-CenterNet adds an angle prediction branch network, which can better handle rotation object detection tasks and achieve a 22.5% detection accuracy improvement. Despite the slightly increased algorithm complexity due to the additional angle prediction branch network and the CBAM compared with the baseline network, the detection speed of the RA-CenterNet algorithm is slightly reduced. However, compared with other algorithms, RA-CenterNet has obvious advantages in both detection accuracy and detection speed.

Fig.5 and Fig.6 present examples of detection results obtained by different algorithms on selected images from the test set. The task of detecting rotated objects is analyzed, and Fig.5 reveals that the Beyond Bounding-Box algorithm faces difficulty in identifying target feature points in datasets with blurred object boundaries due to its reliance on selecting 9 feature points to construct a convex hull, leading to missed detections of frozen targets. On the other hand, the Rotated Faster R-CNN algorithm overcomes this challenge by introducing rotated anchors and corresponding non-maximum suppression (NMS) operations based on the Faster R-CNN architecture. Nevertheless, due to the nature of two-stage detection algorithms, the rotated faster R-CNN algorithm exhibits slower detection speed and false alarms. The oriented RepPoints and SASM algorithms demonstrate no missed detection or false alarms, yet their detection results contain numerous redundant bounding boxes, and their detection speed is comparably slow. Additionally, the

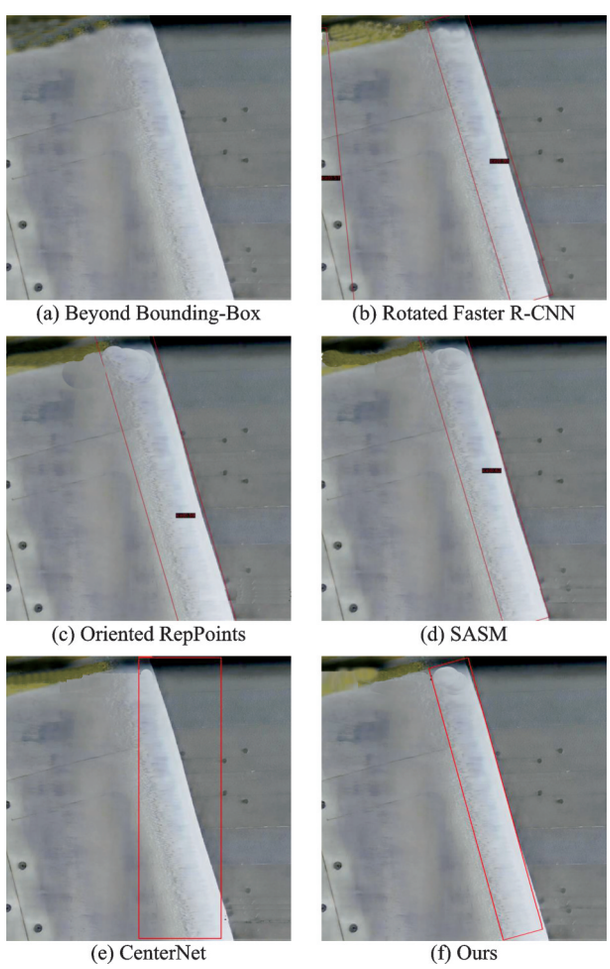

Fig.5 Comparison diagrams of detection results for tilted aircraft wings obtained by different algorithms

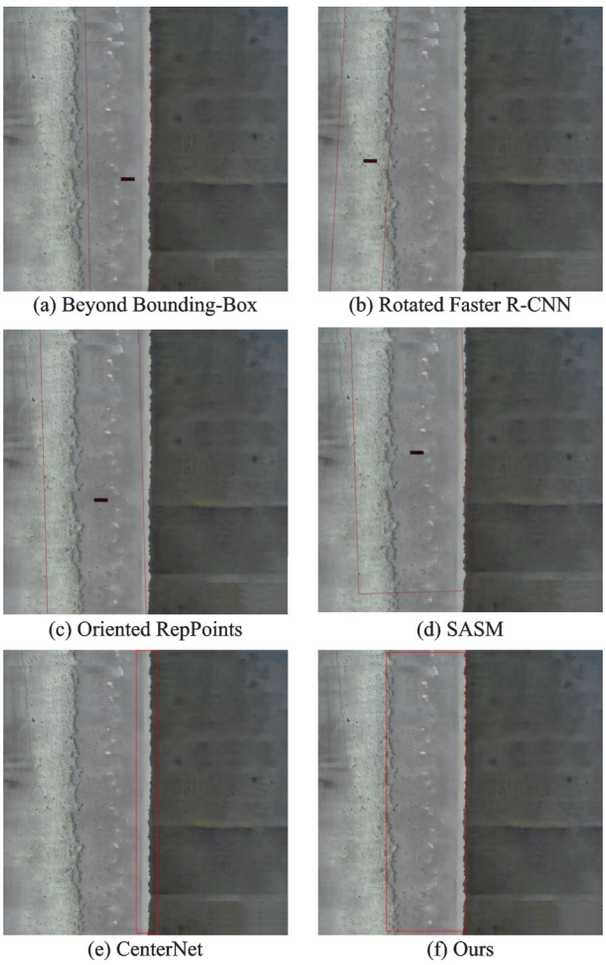

Fig.6 Comparison diagrams of detection results for vertical aircraft wings obtained by different algorithms

CenterNet algorithm detects the frozen area, but its performance in representing the frozen area using horizontal detection boxes is suboptimal due to its design for general object detection tasks. In contrast, the RA-CenterNet algorithm builds upon the success of the CenterNet algorithm in accurately perceiving the target region by adding an angle prediction branch network. This improves the model's ability to learn the orientation of frozen targets, enabling the rectangle box to adjust its angle according to the orientation of the target region and leading to more precise representation of rotated boxes.

Regarding boundary precision, Fig.6 indicates that the Beyond Bounding-Box, Oriented RepPoints, and SASM algorithms detect the frozen area, but the boundaries of the detection boxes exhibit significant deviations. Meanwhile, the detection positions of Rotated Faster R-CNN and CenterNet also deviate significantly from the frozen area. By integrating the CBAM module, the RA-CenterNet algorithm emphasizes the feature information of the target region, such as gradients, and supplies more detailed and effective feature information for the task of frozen target detection. This enables the refinement of the center position and edge position of the detection results, and the precise calibration of the boundaries of the targets in the frozen area.

3.2.2 Ablation experiment results and analysis

To assess the impact of the proposed improvement method on detection network performance, an angle prediction branch network and CBAM module are integrated into the baseline network for experimentation. The experimental results are presented in Table 2.

Table 2 Comparison of experimental results of different modules

Module	Average precision/%	Frame rate/(frame•s^{-1})
CenterNet	70.2	**11.38**
CnterNet+Angle	88.5	9.56
CenterNet+Angle+CBAM	**92.7**	9.47

As indicated in Table 2, the integration of the angle prediction branch network into the model resulted in a substantial 18.3% improvement in detection accuracy relative to the CenterNet algorithm. However, this improvement came at the expense of a slightly reduced detection speed due to the increased complexity of the network. Moreover, the incorporation of the CBAM module into the model with only the angle prediction branch network further improved detection accuracy by 4.2% while maintaining a comparable detection speed.

Fig.7 illustrates the comparison of detection performance after the improvement of different modules. In Fig.7, it is evident that CenterNet can only detect object with horizontal rectangular detection boxes, and the detection area calibration is imprecise. The inclusion of an angle prediction branch network enabled the model to learn the directional factors of icing area targets more effectively, enabling the rectangular boxes to adjust angles based on the

(a) CenterNet (b) CenterNet+Angle (c) CenterNet+Angle+CBAM

Fig.7 Different modules for detecting the effect image

target area's direction. This resulted in rotated boxes, which provide a more accurate representation of the target than horizontal rectangular boxes. However, due to the characteristics of icing targets, there is little difference between the target edge and background information, leading to some deviation in the boundary calibration of the detection boxes.

This paper further incorporates the CBAM module into the model based on the addition of an angle prediction branch network, which facilitates the model to learn the features of icing area targets more effectively, leading to improved boundary calibration of the detection boxes for icing area targets.

4 Conclusions

We propose a method for detecting rotated objects that addresses the challenging task of detecting wing icing targets by utilizing the CenterNet network model. We incorporate an angle prediction branch into the CenterNet network model, which improves its ability to detect objects at various angles and enables successful detection of wing icing targets. Furthermore, we integrate the CBAM module into the feature fusion stage, which enhances the network's ability to focus on the channel and spatial dimensions of icing regions and improves its expression capability in key areas. Experimental results on a wing icing wind tunnel dataset demonstrate that our proposed RA-CenterNet algorithm has a significant competitive advantage over mainstream rotation-based object detection algorithms, with significantly better detection performance than the original CenterNet algorithm. This validates the effectiveness of our proposed improvements. Future work will focus on further improving the detection speed of the RA-CenterNet algorithm while maintaining high accuracy, thus making it applicable to a wider range of detection scenarios.

References

[1] WU Xijun. Aircraft structures and systems[M]. Beijing: Civil Aviation Maintenance Basic Textbook Series, 2020. (in Chinese)

[2] GUO Yanliang. The control technique and experimental research for aircraft hybrid deicing[D]. Wuhan: Huazhong University of Science and Technology, 2017. (in Chinese)

[3] KONG Manzhao, DUAN Zhuoyi, MA Yumin. Study on aerodynamic characteristics of ice accretion in different wing span sections[J]. Journal of Experiments in Fluid Mechanics, 2016, 30(2): 32-37. (in Chinese)

[4] ZHANG Feng, ZHANG Weixin. Research on installation position and height of ice meteorological detector for test aircraft[J]. Science and Technology Innovation Herald, 2020, 17(12): 34-36,38. (in Chinese)

[5] ZHOU X Y, WANG D Q, KRÄHENBÜHL P. Objects as points[EB/OL]. (2019-04-25)[2022-02-01]. https://arxiv.org/abs/1904.07850.

[6] WOO S, PARK J, LEE J Y, et al. CBAM: Convolutional block attention module[C]//Proceedings of the European Conference on Computer Vision (ECCV).[S.l.]:Springer, 2018.

[7] ZHAO Weiwei. Aircraft icing detection system based on piezoelectric materials[D]. Nanjing: Nanjing University of Aeronautics and Astronautics, 2018. (in Chinese)

[8] SHU Jun. Research and experiment of resonant road sensor[D]. Wuhan: Huazhong University of Science and Technology, 2017. (in Chinese)

[9] TAN Shuya, GE Junfeng, YE Lin, et al. Road surface icing detecting system based on multiple sensor[J]. Transducer and Microsystem Technologies, 2016, 35(1): 107-109. (in Chinese)

[10] LI Zhe, WANG Shihao, DONG Zehong, et al. A re-

al-time detection method for ice accumulation on aircraft wings and tailplanes based on image recognition CN202011542206.9[P]. 2021-06-15. (in Chinese)

[11] CHEN Anqiang, DAI Chuan, WANG Wei, et al. A visual icing detection device and aircraft using the device: CN201721739093.5[P]. 2018-07-13. (in Chinese)

[12] MUSCI M A, MAZZARA L, LINGUA A M. Ice detection on aircraft surface using machine learning approaches based on hyperspectral and multispectral images[J]. Drones, 2020, 4(3): 45.

[13] VIOLA P, JONES M J. Robust real-time face detection[J]. International Journal of Computer Vision, 2004, 57: 137-154.

[14] DALAL N, TRIGGS B. Histograms of oriented gradients for human detection[C]//Proceedings of 2005 IEEE Computer Society Conference on Computer Vision and Pattern Recognition (CVPR' 05). [S.l.]: IEEE, 2005.

[15] LOWE D G. Distinctive image features from scale-invariant keypoints[J]. International Journal of Computer Vision, 2004, 60: 91-110.

[16] BAY H, TUYTELAARS T, VAN G L. SURF: Speeded up robust features[J]. Lecture Notes in Computer Science, 2006, 3951: 404-417.

[17] GIRSHICK R, DONAHUE J, DARRELL T, et al. Rich feature hierarchies for accurate object detection and semantic segmentation[C]//Proceedings of the IEEE Conference on Computer Vision and Pattern Recognition. [S.l.]: IEEE, 2014.

[18] GIRSHICK R. Fast R-CNN[C]//Proceedings of the IEEE International Conference on Computer Vision. [S.l.]:IEEE, 2015.

[19] REN S Q, HE K M, GIRSHICK R, et al. Faster R-CNN: Towards real-time object detection with region proposal networks[J]. IEEE Transactions on Pattern Analysis and Machine Intelligence, 2017, 39(6): 1137-1149.

[20] LAW H, DENG J. Cornernet: Detecting objects as paired keypoints[C]//Proceedings of the European Conference on Computer Vision (ECCV). [S.l.]: Springer, 2018.

[21] LIN T Y, MAIRE M, BELONGIE S, et al. Microsoft coco: Common objects in context[C]//Proceedings of European Conference on Computer Vision. Cham: Springer, 2014.

[22] REDMON J, DIVVALA S, GIRSHICK R, et al. You only look once: Unified, real-time object detection[C]//Proceedings of the IEEE Conference on Computer Vision and Pattern Recognition. [S.l.]: IEEE, 2016.

[23] HE K, ZHANG X, REN S, et al. Deep residual learning for image recognition[C]//Proceedings of the IEEE Conference on Computer Vision and Pattern Recognition. [S.l.]: IEEE, 2016.

[24] NEWELL A, YANG K, DENG J. Stacked hourglass networks for human pose estimation[C]//Proceedings of the 14th European Conference on Computer Vision—ECCV 2016. Amsterdam, The Netherlands: Springer, 2016.

[25] YU F, WANG D, SHELHAMER E, et al. Deep layer aggregation[C]//Proceedings of the IEEE Conference on Computer Vision and Pattern Recognition. [S.l.]: IEEE, 2018.

[26] YANG S, PEI Z, ZHOU F, et al. Rotated faster R-CNN for oriented object detection in aerial images[C]//Proceedings of the 2020 3rd International Conference on Robot Systems and Applications. [S.l.]: IEEE, 2020.

[27] GUO Z, LIU C, ZHANG X, et al. Beyond bounding-box: Convex-hull feature adaptation for oriented and densely packed object detection[C]//Proceedings of the IEEE/CVF Conference on Computer Vision and Pattern Recognition. [S.l.]: IEEE, 2021.

[28] HOU L P, LU K, XUE J, et al. Shape-adaptive selection and measurement for oriented object detection[J]. Proceedings of the AAAI Conference on Artificial Intelligence, 2022, 36(1): 923-932.

[29] LI W, CHEN Y, HU K, et al. Oriented reppoints for aerial object detection[C]//Proceedings of the IEEE/CVF Conference on Computer Vision and Pattern Recognition. [S.l.]: IEEE, 2022.

Acknowledgements This work was supported by the Key Laboratory of Icing and Anti/De-icing of China Aerodynamics Research and Development Center (CARDC) (No. IADL20210203), the Natural Science Foundation of Sichuan, China (No.2023NSFSC1393), the Scientific Research Starting Project of Southwest Petroleum University (SWPU) (No.2021QHZ001), and the National Natural Science Foundation of China (No.52006235). All data in this paper are supported by the Key Laboratory of Icing and Anti/De-icing of CARDC. Besides, the authors would like to acknowledge the following people for their assistance: ZHANG Quan, YANG Xinling, WANG Tianfei and WANG Shun.

Authors Dr. **WANG Yifan** received his Ph.D. degree from the University of Sydney, Australia, in 2020. He currently is an assistant professor in School of Computer Science, Southwest Petroleum University. His research interests include human-computer interaction, 3-D reconstruction and

computer vision.

Dr. **ZUO Chenglin** received his Ph.D. degree from National University of Defense Technology, China. He is now an associate researcher at Key Laboratory of Icing and Anti/De-icing of CARDC. His research interests include computer vision, flow visualization and non-contact measurement.

Author contributions Dr. **WANG Yifan** designed the study, compiled the models, and wrote the manuscript. Mr. **WEI Jiatian** designed the model, contributed to the experiments and result analysis and wrote the manuscript. Dr. **ZUO Chenglin** collected the data, designed the model, and contributed to experiment analysis and discussion of the study. Dr. **ZHOU Wenjun** contributed to the design of model and experiment. Dr. **XIONG Hao** collected the data, and contributed to the introduction of the study. Mr. **ZHAO Rong** collected the data, and contributed to the experiments. Prof. **PENG Bo** supervised the research, and optimized the overall model design. Prof. **WANG Yang** supervised the research. All authors commented on the manuscript draft and approved the submission.

Competing interests The authors declare no competing interests.

(Production Editor: SUN Jing)

一种改进的CenterNet机翼结冰检测方法

王一帆[1], 魏家田[1], 左承林[2], 周文俊[1], 熊 浩[2], 赵 荣[2], 彭 博[1], 王 杨[1]

(1.西南石油大学计算机科学学院,成都 610500,中国;
2.中国空气动力研究与发展中心结冰与防除冰重点实验室,绵阳 621000,中国)

摘要:在高空飞行环境下,机翼表面的积冰可能会改变其空气动力学特性并进一步降低升力,因此机翼结冰的检测显得尤为关键。为克服现有积冰检测技术通常依赖于操作人员的经验判断或需要昂贵的工程实施及硬件开发成本的局限,本文提出了一种基于CenterNet模型的旋转目标检测方法RA-CenterNet。针对风洞实验数据集中呈现的特定积冰区域方向问题,设计了一种新颖的角度预测分支网络,有效实现了对旋转目标的精确校准。此外,为了提升神经网络在识别冰形边界时的特征提取能力,研究中还融合了卷积注意力模块(Convolutional block attention module, CBAM)。通过与其他旋转目标检测方法以及基准网络进行的一系列对比实验验证了RA-CenterNet方法的性能。实验结果表明,RA-CenterNet算法在主流的旋转目标检测算法中显示出明显的竞争优势,证明了其在积冰检测领域的应用潜力。

关键词:机翼结冰;深度学习;旋转目标检测;无锚点;注意力机制